Research Paper

Distinct spatial localization of three types of phosphatidyl choline in rat buccal mucosa identified by matrix-assisted laser desorption/ionization imaging mass spectrometry

Mariko Miyagi[1,2], Hana Fukano[1,2], Ryosuke Atsumi[1], Hiroyuki Suzuki[3], Mitsutoshi Setou[2,4,5,6,7], Ikuko Yao[1,4]*

[1] Department of Optical Imaging, Institute for Medical Photonics Research, Preeminent Medical Photonics Education & Research Center, Hamamatsu University School of Medicine, Hamamatsu, Shizuoka 431−3192, Japan
[2] Department of Cellular and Molecular Anatomy, Hamamatsu University School of Medicine, Hamamatsu, Shizuoka 431−3192, Japan
[3] Hiroyuki Dental Clinic of Oral Surgery, 381−11 Hatsuoi-cho, Kita-ku, Hamamatsu, Shizuoka 433−8112, Japan
[4] International Mass Imaging Center, Preeminent Medical Photonics Education & Research Center, Hamamatsu University School of Medicine, Hamamatsu, Shizuoka 431−3192, Japan
[5] Department of Anatomy, The University of Hong Kong, 6/F, William MW Mong Block 21 Sassoon Road, Pokfulam, Hong Kong SAR, China
[6] Division of Neural Systematics, National Institute for Physiological Sciences, National Institutes of Natural Sciences, Okazaki, Aichi 444−0867, Japan
[7] Riken Center for Molecular Imaging Science, Kobe, Hyogo 650−0047, Japan

Abstract The buccal mucosa is an inner lining exposed to frequent friction caused by teeth occlusion and therefore, a vulnerable site to lesions such as stomatitis, leukoplakia, lichen planus and cancer. Although it is considered an important tissue in the field of oral surgery, not enough information regarding the buccal mucosa is available. In this study, we characterized the buccal mucosa in the oral cavity using imaging mass spectrometry (IMS). Tissues such as epithelium, *lamina propria* and muscle were identified in rat buccal mucosa by HE staining. Moreover, IMS data of high-intensity ions were classified into 4 groups according to their distribution. In a previous IMS analysis of mouse tongue tissue, we detected linoleic acid-containing phosphatidyl choline (PC)(diacyl 16:0/18:2), oleic acid-containing PC(diacyl 16:0/18:1) and DHA-containing PC(diacyl 16:0/22:6) as major PCs. In the present work, we analyzed buccal mucosa tissue with emphasis on the aforementioned PC by IMS and showed that the investigated PCs existed in the layers of epithelium, *lamina propria*, and muscle at different ratios. This is the first study to analyze by IMS the buccal mucosa. The results presented here are likely to provide the perspective on understanding oral environments and to develop treatments for oral disorders.

Key words: imaging mass spectrometry, buccal mucosa, phosphatidylcholine, mass microscopy, matrix assisted laser desorption/ionization

* **Corresponding author**
Ikuko Yao
Department of Optical Imaging, Institute for Medical Photonics Research, Preeminent Medical Photonics Education & Research Center, Hamamatsu University School of Medicine, 1−20−1 Handayama, Higashi-ku, Hamamatsu, Shizuoka 431−3192, Japan
E-mail: yaoik@hama-med.ac.jp
Received January 16, 2017. Accepted March 23, 2017.
DOI: 10.24508/mms.2017.06.002

Introduction

Oral mucosa is often afflicted by inflammatory diseases caused by normal oral flora and exposure to external, hygiene-compromised environments[1)]. Although oral mucosa is coated with saliva and protected by the moist environment, the condition is quite unstable due to the external factor. As the entrance of the breathing air and nutrition, it is considered as an important tissue.

Imaging mass spectrometry (IMS) is a technique that can directly analyze molecular distribution on the surface of tissues without previous extraction. In addition, mass spectrometry employing matrix-assisted laser desorption/ ionization (MALDI) can analyze with high sensitivity[2] most lipid classes without major fragmentation. Coupling MALDI with IMS produces the best technique to analyze distribution of lipid molecules in tissues. As a result, a number of lipid analyses by IMS have been reported to date[3].

Using IMS as the analytical tool, we previously characterized tongue[4] and tooth[5] tissues, with emphasis on phospholipids. In the study, we identified and visualized lipid species in mouse tongue tissue by MALDI-IMS. We showed that three types of phosphatidyl choline (PC), namely linoleic acid-containing PC(diacyl 16:0/18:2), oleic acid-containing PC(diacyl 16:0/18:1), and DHA-containing PC(diacyl 16:0/22:6), were located mainly in stratified epithelium, peripheral nerve and muscle as ions at *m*/*z* 758.5, *m*/*z* 760.5, and *m*/*z* 806.5, respectively[4].

Buccal mucosa is the inner lining of cheeks and lips, which are anatomic regions that include all mucous membranes from the opposing line of contact of lips to the mucosa at the line of attachment of the alveolar ridges and the mandibular ridge[6]. Although the buccal mucosa is an important tissue in the oral cavity, there is not enough information about the buccal mucosa, and no IMS analysis of buccal mucosa has been previously conducted. Here we for the first time attempted to build the basis of IMS for buccal mucosal tissue, especially focused our analysis on the three types of PCs we previously visualized in mouse tongue tissue [i.e., PC(diacyl 16:0/18:2), PC(diacyl 16:0/18:1) and PC(diacyl 16:0/22:6)].

Material and Methods

Animals

Adult female Wister rats were purchased from SLC (Hamamatsu, Japan) and given *ad libitum* standard diet and water. The care and use of laboratory animals were conducted in accordance with the Animal Experiment Regulations issued by the Hamamatsu University School of Medicine, which follows the *Guidelines for the proper Conduct of Animal Experiments* approved by the Science Council of Japan.

Chemicals and reagents

Indium-tin-oxide (ITO)-coated Glass slides [13-mm square conductive ITO-coated (100 Ω slides)] were purchased from Matsunami Glass Ind., Ltd. (Osaka, Japan). 2,5-dihydroxybenzoic acid (DHB) was purchased from Bruker Daltonics (Bremen, Germany). All chemicals used in this study were of the highest purity available.

Preparation of rat buccal mucosa tissue sections

Rats were anesthetized and decapitated afterward. The center of the head was incised and the surface of one side of the buccal mucosa was visually exposed. Next, the tooth cervix was carefully peeled off from the border to isolate buccal mucosal tissue. After those procedures, buccal mucosa were cut and removed.

All samples damaged by cuts or long exposure to ambience during processing were excluded. Buccal mucosal samples were embedded in 4% carboxymetyl cellulose (CMC), submerged in *n*-hexane and frozen with dry ice within 5 min after decapitation.

Processed samples were then stored at −80°C with no fixation. Next, tissues were sliced into 10-μm sections using a cryostat (Cryostat CM 1850; Leica Microsystems, Wetzlar, Germany) with the chamber temperature at −20°C. For IMS analysis, the tissue sections were mounted onto ITO-coated glass slides. All slides with mounted sections were stored at −20°C until further use.

Matrix application

A matrix solution was prepared by dissolving 50 mg of DHB in 1 mL of methanol/water (7:3, v/v) with 125 mM ammonium sulfate. DHB matrix solution was sprayed uniformly at a distance of 15 cm from the tissue surface with an airbrush equipped with a 0.2-mm nozzle. In total, 2 mL of DHB matrix solution was sprayed on each slide. DHB is a common matrix used to ionize lipids by MALDI−IMS in the positive ion mode. Ammonium sulfate was added to the matrix solution in order to form positive ions of $[M+H]^+$, but not of $[M+Na]^+$and $[M+K]^+$, which helped reduce overlapping of signals from different molecules. After glass slide-mounted tissue sections were dried, they were analyzed by attaching the glass slides to the MS microscope holder.

Imaging mass spectrometry

MALDI−IMS analysis was couducted using iMScope, a MS microscope (Shimadzu, Kyoto, Japan). Data were acquired in the positive ion mode with a 50-μm pitch. The

analysis conditions were: laser irradiation time, 200 shots; frequency, 1000 Hz; illumination diameter, minimum (5 μ m); laser power, 30%; and mass range, 600 to 1000. A mass range setting of 400 to 1000 resulted in failure, due to noise signals in the data. Imaging MS Solution software (Shimadzu) was used to create two-dimensional ion-density maps. After analysis by MALDI−IMS, glass slide-mounted tissue sections were immersed in acetone for 5 s to wash the matrix off tissues, and stained with hematoxylin-eosin (HE) afterward.

Results and Discussion

Morphology and histology of rat mucosa tissue

Prior to IMS analysis, we validated the morphology and histology of rat mucosal tissue (Fig. 1). An image of rat buccal tissue prior to separation of the mucosa and other surrounding tissues is shown in Fig. 1a. The surface of buccal mucosa tissue was smooth and with a gray-purple color. After removal, the buccal mucosal tissue and the muscle shrunk and thickened due to loss of attachment to the surrounding tissues. In the HE-stained buccal mucosal tissue, layers of epithelium, *lamina propria*, and muscle were observed, which were histologically similar to that of human, although the epithelium was thicker than that found

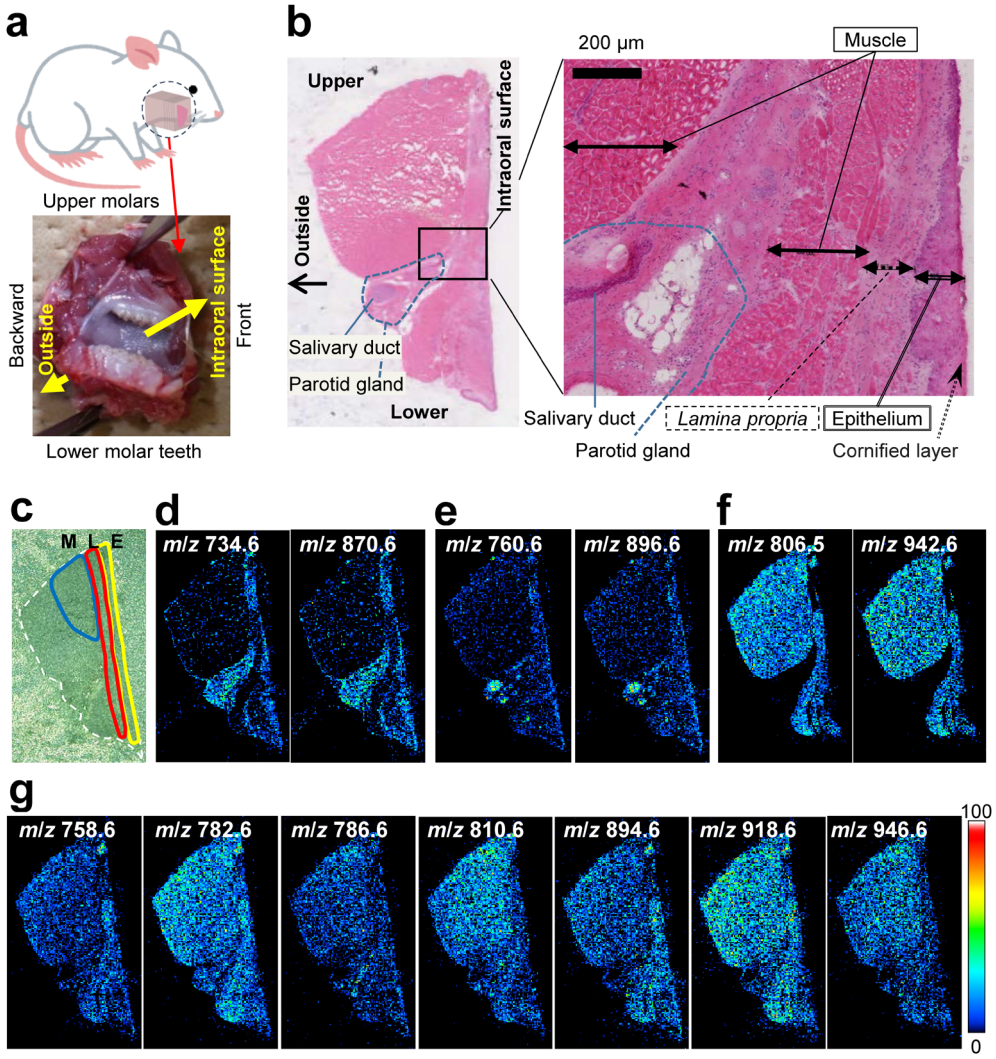

Fig. 1. Optical and ion mages of rat buccal mucosal tissue.
(a) Image of rat buccal tissue prior to separation of the mucosa tissue and other surrounding tissues. (b) HE-stained tissue section of rat buccal mucosa. After imaging mass spectrometry (IMS) analysis, the same section was subjected to HE staining. The right panel shows a high magnification image, and the epithelium, *lamina propria*, and muscle can observed. Cornified layer can be seen on the edge. (c) Optical image of the same section analyzed by IMS. Muscle (M), Lamina propria (L), and Epithelium (E) areas were determined by visual observation for re-analysis by Imaging MS Solution™. (d−g) Reconstructed ion images with high intensity in each layer of buccal mucosa.

Table 1. List of major ions and their intensities detected in each analyzed region of interest

No.	Muscle		Laminapropria		Epithelium		Matrix	
	m/z	Intensity	*m/z*	Intensity	*m/z*	Intensity	*m/z*	Intensity
1	782.5	1,349,435	782.5	1,204,431	782.5	718,973	681.1	2,760,634
2	806.5§	1,217,318	806.5§	871,982	760.6*	676,456	637.0	1,468,609
3	810.6	1,134,766	758.5#	868,018	758.5#	660,100	682.1	1,088,642
4	758.5#	875,041	810.6	700,867	681.1	626,310	817.1	865,282
5	918.6	711,437	760.6*	674,228	734.5	506,647	698.1	760,590
6	786.6	671,377	918.6	599,040	896.6	461,728	639.0	684,443
7	783.5	652,758	783.5	567,330	894.6	412,153	619.0	668,620
8	946.6	649,585	894.6	520,215	806.5§	360,392	638.0	604,380
9	942.6	634,826	734.5	504,391	810.6	353,496	716.1	601,667
10	807.5	601,907	786.6	457,348	786.6	353,244	692.9	548,102
11	760.6*	599,772	896.6	453,831	870.6	347,305	624.9	529,043

The top 11 ions in each regions of interest (ROI) are listed. The ions investigated in this study are underlined and ions at *m/z* 758.5, 760.5, and 806.5 are indicated by #, *, and §, respectively.

in human oral cavity (Fig. 1b). In addition, keratinocytes or somewhat cornified cells were observed on the edge where lower molars touched (Fig. 1b). Cornification is believed to have been caused by daily friction because no other causes of inflammation such as lymphocytes infiltration[6,7] were detected. The tissue section contained part of the salivary duct (Fig. 1b), Thus, we believed the tissue section also contained the parotid gland which is a major salivary gland located along the cheek muscle[8].

Distributions of major ions detected in the buccal mucosa

The region of interest (ROI) corresponding to the three layers of muscle, *lamina propria*, and epithelium were chosen in images of matrix-applied samples, based on the image of HE staining (Fig. 1c). In the three ROIs, the 16 ion species were included in the top 11 ions (Table 1) and images of 13 ion species out of 16 were reconstructed (Fig. 1c−f). Ions at *m/z* 783.5 and 807.6 were omitted because they were isotopes of ions at *m/z* 782.5 and 806.5, respectively. The ion at *m/z* 681.1 was not analyzed because it was derived from the matrix (Table 1). Ion images were roughly classified into four groups judged by the distribution. For example, ions at *m/z* 734.5 and 870.6 observed in the parotid gland tissue and the surface area with a gradual increase in intensity of their signals on the surface were classified into one group (Fig. 1d). Ions at *m/z* 760.6 and 896.6 widely distributed in the salivary duct and the surface layer were allocated into another group (Fig. 1e). Ions at *m/z* 806.5 and 942.6 observed in the muscle were classified into yet another group (Fig. 1f). Lastly, ions at *m/z* 758.5, 786.5, 810.6, 894.6, 918.6, and 946.6, as well as the ion at *m/z* 782.5, with the highest signal intensity in all three ROI, were classified into the final group. All ions in this final group were widely distributed throughout the entire ROI of the tissue section (Fig. 1g).

Based on data from previously reported studies, including our previous IMS analysis of mouse tongue tissue[4,9], ions at *m/z* 758.5, 760.6, and 806.5, detected on buccal mucosal tissue (Table 1), were regarded as [PC(diacyl 16:0/18:2)+H]+(*m/z* 758.5), [PC(diacyl 16:0/18:1)+H]+(*m/z* 760.6), and [PC(diacyl 16:0/22:6)+H]+(*m/z* 806.5). Similarly, other ions among those listed in Table 1 were identified by their *m/z* values and data from previously reported IMS analyses. For example, the ion at *m/z* 782.5 with a broad distribution was identified as PC(16:0/20:4)+H[4]. Moreover, we considered ions at *m/z* 734.5, 786.6 and 810.5 as PC(16:0/16:0)+H, PC(18:0/18:2)+H, and PC(18:0/20:4)+H, respectively[4].

Ion images of three PCs in buccal mucosa

Reconstructed images of [PC(diacyl 16:0/18:2)+H]+(*m/z* 758.5), [PC(diacyl 16:0/18:1)+H]+(*m/z* 760.6), and [PC(diacyl 16:0/22:6)+H]+(*m/z* 806.5) are shown in Fig. 2a−d and their higher magnification of these images can be seen in Fig. 2e−h. PC(16:0/18:2) was broadly distributed throughout the analyzed tissue and partly accumulated in the layer around the intraoral surface (Fig. 2a, e).

PC(16:0/18:1) produced signals on the surface layer of the buccal mucosa and glandular area with a particularly strong signal in the salivary duct (Fig. 2b, f). PC(16:0/22:6) was homogeneously distributed, except for the surface and glandular tissue areas (Fig. 2c, g). Finally, a merged image showed that the aforementioned PCs were differently distributed in the same tissue section (Fig. 2d, h). These IMS results clearly showed that the investigated PCs were differently distributed in each layer.

PC(16:0/18:2) at *m*/*z* 758.5, which had the highest intensity in the stratified epithelium of mouse tongue analysis[4], was widely distributed in the ROI of the buccal mucosa (Fig. 2). PC(16:0/18:1) at *m*/*z* 760.6, which was abundant in the peripheral nerve of the mouse tongue[4], was observed on the surface area of buccal mucosa, salivary duct, and glandular area. It is worth mentioning that the signal detected in the salivary duct was particularly high, which suggests that PC(16:0/18:1) at *m*/*z* 760.6 is a major PC in the nervous system and gland tissues. PC(16:0/22:6) at *m*/*z* 806.5 was located in the muscle tissue in both in the tongue and buccal mucosa, suggesting that it is a common PC not only in oral tissue but also in other organs.

Comparison of the distributions of three PCs in rat buccal mucosa

The average intensity of the aforementioned PCs in rat buccal mucosa was calculated (Fig. 2i). As shown in Fig. 2i, the correlation of values were in agreement with the images of PCs detected in the same tissue section as shown in Fig. 2i, in particular in images taken at higher magnification. For example, PC(16:0/18:2) at *m*/*z* 758.5 had a relatively uniform intensity in all tissues except for the epithelium where the signal decreased. The intensity of PC(16:0/18:1) at *m*/*z* 760.6 increased on the surface of the epithelium and was the strongest. The intensity of PC(16:0/22:6) at *m*/*z* 806.5 was notably high in the muscle, markedly reduced in the lamina propria, and the lowest in the epithelium area (Fig. 2c). Focusing on global patterns, we compared the average mass spectrum of each ROI (Fig. 2j).

In the previous our report, it was found that the spectral patterns obtained in the analysis of muscle, stratified epithelium, and the peripheral nerve of tongue tissue were quite different from each other[4]. In contrast, no large differences between spectral patterns were observed in the present analysis of buccal mucosa. It can be suggested that averaged spectrum were observed in this study because the analyzed area selected in buccal mucosa was smaller than that in tongue and the small ROI contained more than one kind of tissue structures.

Comparison of major ions in buccal mucosal tissue with those of previous reports

Ions detected in buccal mucosal tissue (Table 1) were compared with molecules reported in past IMS analyses. Warthin tumor (War-T), the second most common benign parotid gland tumor, consists mainly of neoplastic epithelium and lymphoid stroma[10]. We found that ions detected in the present study at *m*/*z* 758.5, 760.6, 806.5, 734.5, 782.5, 786.6, and 810.6 were also reported in War-T tissue sections as K+adducts at *m*/*z* 796.5, 798.5, 844.5, 772.5, 820.5, 824.5, and 848.5, respectively[10]. Of these, ion at *m*/*z* 796.5 in regions of War-T tissue had a lower level than did those detected in non-War-T tissue, but the ion at *m*/*z* 897.5 had almost matching levels in both tissues. In contrast, other ions, especially *m*/*z* 772.5 and *m*/*z* 824.5, were higher in War-T tissue than in non-War-T tissue[10]. The signal of PC(16:0/16:0) + K at *m*/*z* 772.5, which was localized mainly in lymphoid stroma with a high intensity at the *follicului lymphaticus* in the War-T tissue[10], corresponded to the H+adduct at *m*/*z* 734.6, which was detected in glandular tissue in the present study. This result may indicate that PC(16:0/16:0) is abundant in cells that are involved in secretion. The ion at *m*/*z* 884.5 was observed in regions of both neoplastic epithelium and lymphoid stroma in War-T tissue and it was identified as PC(18:2/20:4) by MS/MS analysis. Nonetheless, although the *m*/*z* value corresponded to the H+adduct at *m*/*z* 806.5, the PC species detected in War-T tissue may be different from those detected in present study. In this study, we theorize that the ion at *m*/*z* 806.5 is PC(16:0/22:6), which was previously identified by MS/MS in tongue tissue[4] and it is also commonly found in muscle tissue. As it was in the present study, the ion at *m*/*z* 782.5 was reported in a previous IMS analysis of tooth tissue[5], although PC(diacyl 16:0/18:2), PC(diacyl 16:0/18:1) and PC(diacyl 16:0/22:6) were not detected. The ion at *m*/*z* 782.5 was also detected in tongue tissue[4]. We theorize that this molecule commonly exists in large amounts in oral tissues. In the present study we did not detect the ion at *m*/*z* 469.3, perhaps due to noise signals detected in the analysis at a *m*/*z* range of 400 to 1000 (data not shown; see also the Materials and Methods section). While lysoPC was found

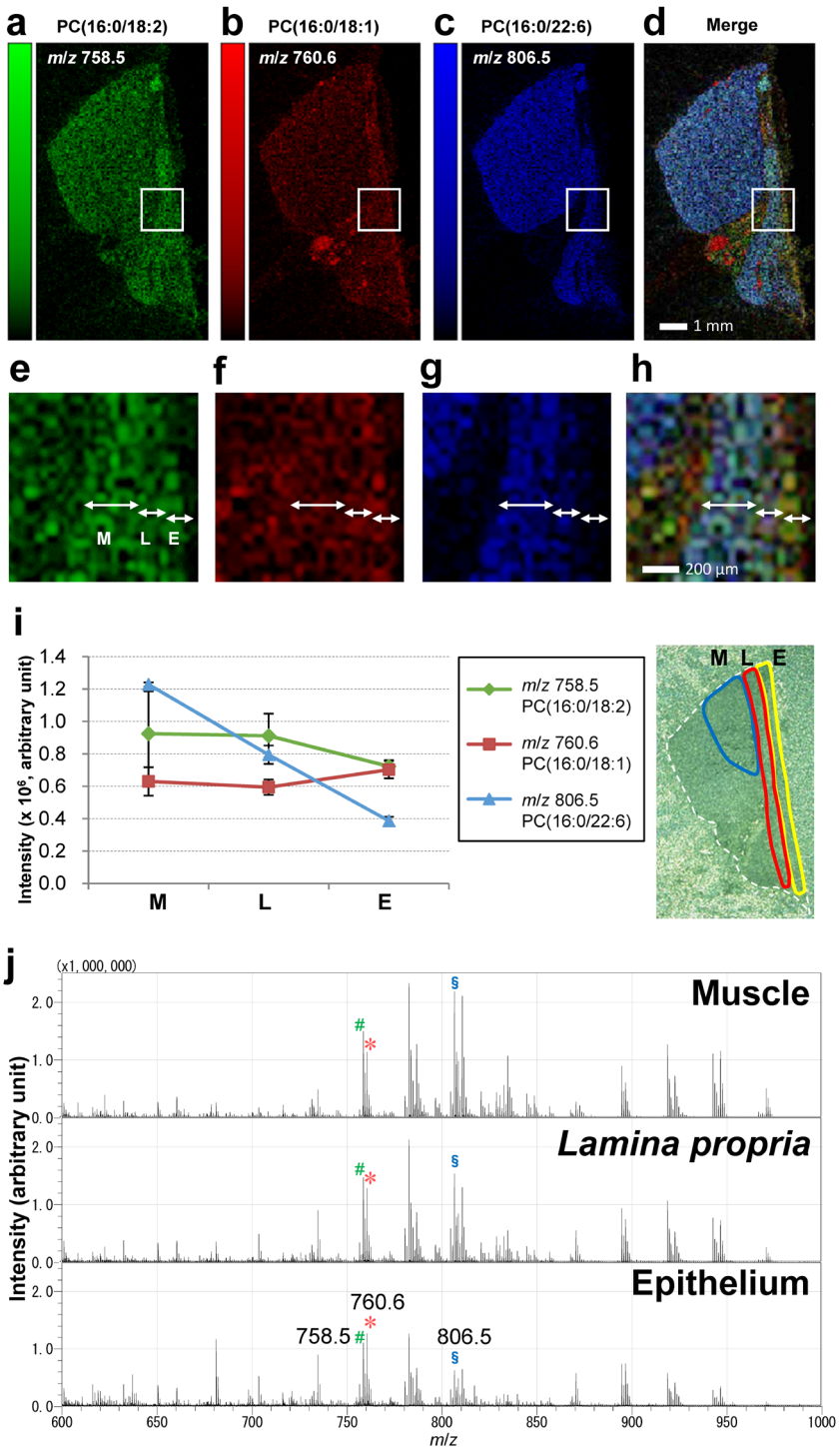

Fig. 2. Specific distributions of the investigated PCs in the buccal mucosal tissue.
(a–c) Images of ions at *m/z* 758.5, 760.5, and 806.5. (d) Merged image; Green, ion at *m/z* 758.5 for PC(diacyl 16:0/18:2)+H; Red, ion at *m/z* 760.5 for PC(diacyl 16:0/18:1)+H; Blue, ion at *m/z* 806.5 for PC(diacyl 16:0/22:6)+H. PC showed different distributions. (e–h) High magnification images of a–e. Hatched areas were zoomed out. The ion at *m/z* 758.5 was broadly distributed, the ion at *m/z* 760.5 was found throughout most surface layer with a strong signal at the salivary duct, although fewer signals of the ion at *m/z* 806.5 were observed on the outer layer. (i) Signal intensity of ions of the investigated PC in each area in tissues from six different rats. Investigated PC were distributed with different populations in each layer. Values indicating signal intensity are the means±SEM (n=6) (j) Comparison of mass spectra obtained from each area of muscle; *lamina propria*; and epithelium. The peaks of ions at *m/z* 758.5, 760.5, and 806.5 are indicated by #, * and §, respectively. M, Muscle; L, *Lamina propria*; E, Epithelium.

at *m*/*z* 469.3 in inflamed tissues of a rat periodontal disease model[5], the reason for the lack of detection of this ion in the investigated tissues in the present study may be due to our usage of buccal mucosal tissue of healthy rats. Detection of such inflammation markers will contribute to diagnose or confirm the effect of remedy and periodontal surgery.

Contribution to the development of treatments for disorders

Buccal mucosa is the recurrent site for lichen planus and leukoplakia, which are associated with a risk of cancer development. At present, it is common to assay oral lesions by using tissue samples excised from sites with suspected pathological signs, which also include adjacent normal tissue. If an IMS reference database of oral tissues is established, it can be reasonably predicted that the sample size of tissues would be reduced, and samples would be eventually deemed unnecessary. Recently developed technique seems to support this assertion. Indeed, emerging rapid evaporative ionization mass spectrometry (REIMS) permits near-real-time characterization of human tissue in vivo by analysis of aerosol released during electrosurgical dissection and the electrosurgery with REIMS for tissue diagnostics is known as the intelligent knife (iKnife)[11,12]. A reference database of IMS across a wide range of tissues could also help discriminate between normal and cancer tissues. It can be predicted that the establishment of an IMS database of oral tissues could help reduce and even eliminate the need for tissue sampling. In addition, a reference database of IMS across a wide range of tissues would help advance the development and diagnosis power of emerging techniques such as REIMS.

Conclusion

In conclusion, to the best of our knowledge this is the first work to report an IMS analysis of buccal mucosal tissue. We visualized by MALDI−IMS PC(diacyl 16:0/18:2), PC(diacyl 16:0/18:1) and PC(diacyl 16:0/22:6) in rat buccal mucosal tissue. We also showed that these PCs had distinct localizations and populated each layer of the buccal mucosa at different levels. The results presented here may provide the basis for further research in order to gain a deeper understanding of the biology of the buccal mucosa and the oral environment and contribute to the development of treatments for disorders such as oral mucositis.

Acknowledgements

This study was supported by MEXT KAKENHI Grant Number JP 24111547 and JSPS KAKENHI Grant Numbers JP26460388, JP16KT0134C1, JP26670461C1, JP15H05898B1, Imaging Platform Grant Number 967, CREST from AMED Grant Number 921910520.

References

1) Uchiyama Y, Hayasaka T, Masaki N, Watanabe Y, Masumoto K, Nagata T, et al: Imaging mass spectrometry distinguished the cancer and stromal regions of oral squamous cell carcinoma by visualizing phosphatidylcholine (16:0/16:1) and phosphatidylcholine (18:1/20:4). *Anal Bioanal Chem* 406(5): 1307−1316, 2014.
2) Zaima N, Hayasaka T, Goto-Inoue N, Setou M: Imaging of metabolites by MALDI mass spectrometry. *J Oleo Sci* 58(8): 415−419, 2009.
3) Zaima N, Sasaki T, Tanaka H, Cheng XW, Onoue K, et al: Imaging mass spectrometry-based histopathologic examination of atherosclerotic lesions. *Atherosclerosis* 217(2): 427−432, 2011.
4) Enomoto H, Sugiura Y, Setou M, Zaima N: Visualization of phosphatidylcholine, lysophosphatidylcholine and sphingomyelin in mouse tongue body by matrix-assisted laser desorption/ionization imaging mass spectrometry. *Anal Bioanal Chem* 400(7): 1913−1921, 2011.
5) Hirano H, Masaki N, Hayasaka T, Watanabe Y, Masumoto K, et al: Matrix-assisted laser desorption/ionization imaging mass spectrometry revealed traces of dental problem associated with dental structure. *Anal Bioanal Chem* 406(5): 1355−1363, 2014.
6) Sagheb K, Blatt S, Kraft IS, Zimmer S, Rahimi-Nedjat RK, et al: Outcome and cervical metastatic spread of squamous cell cancer of the buccal mucosa, a retrospective analysis of the past 25 years. *J Oral Pathol Med*: Offi Pub Int Assoc Oral Patho AAOP, 2016.
7) Tang J, Han Y, Zhang F, Ge Z, Liu X, et al: Buccal mucosa repair with electrospun silk fibroin matrix in a rat model. *Int Artif Organs* 38(2): 105−112, 2015.
8) Treuting P, Dintzis S (eds) *Comparative anatomy and histology: A mouse and human atlas*. 461 pp, Academic Press, Oxford, UK, 2012. ISBN: 978-0-12-381361-9. *Vet Pathol* 49(5): 886, 2012.
9) Ishikawa S, Tateya I, Hayasaka T, Masaki N, Takizawa Y, et al: Increased expression of phosphatidylcholine (16:0/18:1) and (16:0/18:2) in thyroid papillary cancer.

PloS ONE 7(11): e48873, 2012.

10) He Q, Takizawa Y, Hayasaka T, Masaki N, Kusama Y, et al: Increased phosphatidylcholine (16:0/16:0) in the folliculus lymphaticus of Warthin tumor. *Anal Bioanal Chem* 406(24): 5815−5825, 2014.
11) Alexander J, Gildea L, Balog J, Speller A, McKenzie J, et al: A novel methodology for in vivo endoscopic phenotyping of colorectal cancer based on real-time analysis of the mucosal lipidome: A prospective observational study of the iKnife. *Surg Endosc* 31(3): 1361−1370, 2017.
12) Balog J, Sasi-Szabo L, Kinross J, Lewis MR, Muirhead LJ, et al: Intraoperative tissue identification using rapid evaporative ionization mass spectrometry. *Sci Transl Med* 5(194): 194ra93, 2013.